Ethylene and 1-Hexene Sorption in LLDPE under Typical Gas-Phase Reactor Conditions: Experiments

Antonin Novak,[1] Marek Bobak,[1] Juraj Kosek,[1] Brian J. Banaszak,[2*] Dennis Lo,[2†] Tomy Widya,[2‡] W. Harmon Ray,[2] Juan J. de Pablo[2]

[1]*Department of Chemical Engineering Prague Institute of Chemical Technology, 166 28 Prague, Czech Republic*
[2]*Department of Chemical and Biological Engineering University of Wisconsin, Madison, Wisconsin 53706, USA*

Received 19 October 2004; accepted 19 October 2004
DOI 10.1002/app.23508
Published online in Wiley InterScience (www.interscience.wiley.com).

ABSTRACT: The sorption of ethylene and 1-hexene and their mixture in three poly(ethylene-*co*-1-hexene) samples is measured gravimetrically at temperatures 70, 90, and 150°C and pressures 0–30 bar. Gravimetric sorption measurements are supplemented with microscopic observations of swelling of polyethylene particles caused by sorption and the extent of swelling is found to be significant. Experimental data are compared with predictions of PC-SAFT (perturbed chain—statistical associating fluid theory) equation of state. Comparison of sorption data in semicrystalline polymer (measured at 70 and 90°C) and amorphous polymer (at 150°C) demonstrates the constraining effect of semicrystalline structure. Solubilities of penetrants in investigated samples are not observed to depend on the content of 1-hexene in copolymers. The solubility of the mixture of ethylene and 1-hexene is smaller than the sum of solubilities of individual components at 70 and 90°C. © 2006 Wiley Periodicals, Inc. J Appl Polym Sci 100: 1124–1136, 2006

Key words: polyethylene; swelling; phase behavior; thermodynamics

INTRODUCTION

Sorption equilibria of reactants and diluents in polyolefins affect not only reaction rates in catalytic polymerization of olefins, but are important also in the down-stream processing of produced particles, e.g., in the degassing operation. Unreacted monomers (e.g., ethylene or propylene) and comonomers (e.g., 1-butene, 1-hexene) have to be removed from the produced polymer particles in the degassing unit. The knowledge of solubility and transport properties of monomer(s) in polyolefins is necessary for the optimal design and operation of degassing units and for the successful transfer of kinetic data from laboratory liquid-slurry reactors to pilot plant gas-dispersion reactors.

Correspondence to: J. Kosek (Juraj.Kosek@vscht.cz).
**Present address:* BASF AG, GKE, 67056 Ludwigshafen, Germany.
†*Present address:* DuPont Surfaces R&D, Buffalo, NY 14207.
‡*Present address:* Department of Chemical Engineering and Materials Science, University of Minnesota. Minneapolis, MN 55455.

Contract grant sponsor: Czech Grant Agency; contract grant number: 104/02/0325 and 104/03/H141.
Contract grant sponsor: Ministry of Education; contract grant number: MSM 6046137306.

The commonly observed enhanced reaction rate of ethylene polymerization after the addition of 1-hexene was traditionally explained by the coordination chemistry of ligands on the central metal of the catalyst.[1,2] Alternatively, this increase in the reaction rate could be partially attributed to the enhanced solubility and diffusion of ethylene in amorphous polymer phase caused by the cosorption of 1-hexene, as demonstrated in this article.

In the catalytic polymerization of olefins is the dependence of reaction rate of chain propagation R_p on temperature T usually considered to have the Arrhenius form

$$R_p \sim k_{p0} \exp(-E_a/(RT)) c_M^{\text{am. pol.}} \quad (1)$$

where we have neglected the monomer transport resistance in the polymer phase. Here k_{p0} is the preexponential factor, E_a is the activation energy, R is the gas constant and $c_M{}^{\text{am.pol.}}$ is the concentration of monomer in the amorphous polymer phase, which is considered to be in the sorption equilibrium with the bulk concentration of monomer $c_M{}^{\text{bulk}}$

$$c_M^{\text{am. pol.}} = f^{\text{sorp}}(c_M^{\text{bulk}}, T) \quad (2)$$

For a monomer such as ethylene where Henry's law can apply, $c_M{}^{\text{am.pol.}} = k_{\text{Eth}}{}^{\text{sorp}}(T)\, c_M{}^{\text{bulk}}$, the rate expression (1) can be written in the form

$$R_p \sim k'_{p0} \exp(-E'_a/(RT)) c_M^{\text{bulk}} \quad (3)$$

where k'_{p0} is the apparent preexponential factor and E'_a is the apparent activation energy, which includes the effect of temperature dependence of sorption equilibrium of monomer in the amorphous polymer. Thus, it is important to distinguish between the purely kinetic and apparent activation energies E_a and E'_a when processing experimental results of kinetic measurements. In the case of copolymerization, we can similarly differentiate between the kinetic reactivity ratios evaluated from the concentration of monomers in the amorphous polymer and the apparent reactivity ratios based on the composition of the gas phase. The framework of the multigrain model of the growing polyolefin particle is often adopted for the discussion of sorption, transport and reactions processes.[3]

Membrane separations employing the compact polyolefin membranes are another field of research and industrial application that generates considerable interest in the sorption equilibria and the transport of species in polymers, particularly in the cosolubility effects of various species in membranes.

Sorption equilibria of sparingly soluble solutes (e.g., ethylene, nitrogen, CO_2) in polyolefins at common pressures can be described by the linear Henry's law.[4–8] However, sorption isotherms of these gases can be nonlinear in the region of high pressures, e.g., the slope of CO_2 isotherm in HDPE and PP increases moderately with pressure, whereas that for nitrogen slightly decreases with pressure.[9]

The solubility of most gases and vapors in polyolefins decreases with temperature except that of gases with low critical temperature, such as nitrogen and hydrogen, which show the so-called "reverse solubility" at elevated temperatures, where the solubility increases with temperature.[6,9] The measurement of the temperature dependence of the sorption of ethylene, 1-hexene, and their mixture in several samples of LLDPE is one of the objectives of this work.

Sorption isotherms of ethylene in polyolefins are linear, but sorption isotherms of higher α-olefins (e.g., propylene, 1-butene, 1-hexene) are nonlinear, and the mass of sorbed penetrants can be an order of magnitude or more larger than that reported for the sorption of ethylene.[8,10,11] The sorption of penetrant species occurs only in the amorphous phase of semicrystalline polyethylene.[4,5,12] Hence, the solubilities of species are often reported as the mass of sorbed penetrant per the unit mass of the amorphous polymer. However, the sorption characteristics in the amorphous domain of semicrystalline polymer are not the same as those in a totally amorphous polymer, and the solubility of species in the amorphous phase generally decreases with increasing crystallinity.[8,10] This decrease of the solubility with increasing crystallinity was suggested to be caused by the presence of crystalline regions that impose the constraints on polymer chains in the amorphous phase,[13] so that there is a limited extent of swelling of amorphous regions constrained elastically by the crystalline domains.[12,14] Kiparissides et al.[15] found that the solubility of ethylene at temperatures 50, 60 and 80°C in HDPE reached a maximum value at pressure of about 50 bar and attributed this behavior to the limited degree of swelling of amorphous PE phase constrained by the crystalline PE. However, the idea of limited swelling has not been confirmed by direct measurements of the swelling or limited sorption and/or swelling by other solutes than ethylene. The detailed analysis of the elastic constraining effect using the PC-SAFT equation of state has been conducted by Banaszak et al.[16] who estimated that ~20–30% of chains in the amorphous phase were affected by the constraining effect at the 60–70% crystallinity of the investigated poly(ethylene-*co*-1-hexene) samples.

A limited amount of sorption data reporting the dependence on the composition of ethylene copolymers is available. Yoon et al.[17] measured the solubility of ethylene, propylene, and 1-butene in random poly(ethylene-*co*-propylene) and poly(ethylene-*co*-1-butene) copolymers at temperatures 30–90°C and pressures up to 1.3 bar. At this low pressure, the solubilities of ethylene and propylene were found to be nearly independent of the copolymer composition; however, the solubility of 1-butene depends on the composition of poly(ethylene-*co*-1-butene) copolymers, especially at lower temperatures.

Solubility data of multicomponent gas mixtures ethylene + higher α-olefin (+ diluent) in polyolefins at typical reaction conditions are the subject of interest in the polyolefin industry. The questions formulated in this respect are: (i) is the total sorption of the gas mixture equal to the sum of gas sorptions of individual components and (ii) does the presence of higher α-olefin enhance or lower the solubility of ethylene?

Hutchinson and Ray[12] pointed out that, for the sorption measurements of Robeson and Smith[18] and Li and Long,[19] the solubility of the mixture of components is larger than the sum of solubilities of pure components. Li and Long[19] measured the solubility of pure ethylene and methane as well as their mixture in LDPE at temperature 25°C and pressure up to 80 bar. Robeson and Smith[18] reported the sorption of ethane/butane mixtures of different compositions in LDPE at atmospheric pressure and temperatures 30–60°C.

Sorption isotherms for ethylene/1-hexene mixtures in LLDPE at common polymerization conditions of the gas phase processes have not been reported yet. Only a limited number of experimental studies of phase equilibria in ternary systems at elevated temperatures and pressures are available with the exception of measurements of Yoon et al.[17] conducted at low pressures, cf. Table I. Yoon et al.[17] measured gravimetrically the solubility of ethylene/propylene

TABLE I
Survey of Experimental Studies of Sorption Equilibria of Gas Mixtures in Polyethylene

Authors	System	Conditions
Yoon et al.[17]	Ethylene/propylene/EP copolymer	50–90°C; 0.3–1.5 bar
Kennis et al.[21]	*n*-Hexane/nitrogen/HDPE	120–180°C; up to 75 bar
Chan and Radosz[22]	Ethylene/1-hexene/PE	up to 180°C; up to 1400 bar
Dörr et al.[20]	Ethylene/(He, N_2, CO_2, CH_4, C_2H_6,C_3H_8, C_4H_{10}, C_6H_{12})/PE	120–220°C; up to 220 bar
Chen et al.[23]	Ethylene/*n*-hexane/LLDPE	100–200°C; up to 200 bar

mixture of varying composition in poly(ethylene-*co*-propylene) copolymer containing 48.4 mol % of ethylene. The authors found that the solubility of the mixture of gases was higher than that estimated from the independent solubilities of pure components, especially at the higher partial pressure of propylene.

Other researchers measured cloud points of ternary mixtures in high-pressure autoclaves. Dörr et al.[20] found that inert gases like helium, nitrogen, methane, and CO_2 increase the cloud point of the ethylene/polyethylene mixture and, therefore, decrease the solubility of ethylene in polyethylene. Thus, these inert gases act as antisolvents. On the contrary, species like ethane, propane, *n*-butane, and 1-hexene increase the solubility of ethylene in polyethylene and act as cosolvents. Moreover, Dörr et al.[20] demonstrated that nitrogen acts as an antisolvent also in the case of high-pressure phase equilibria in the system ethylene/1-hexene/poly(ethylene-*co*-1-hexene). Similarly Kennis et al.[21] found that nitrogen has an antisolvent effect in the mixture N_2/*n*-hexane/HDPE. Chan and Radosz[22] and Chen et al.[23] found the antisolvent effect of ethylene in systems ethylene/1-hexene/polyethylene and ethylene/*n*-hexane/metallocene-LLDPE, respectively.

Both Monte-Carlo molecular and equation of state (EOS) simulations of the ethylene/1-hexene/polyethylene system at typical gas-phase polymerization conditions were conducted by Nath et al.[24] who employed the SAFT EOS[25–28] and by Banaszak et al.[16] who used the improved PC-SAFT EOS.[29–31] Simulation results showed that ethylene acts as an antisolvent, whereas 1-hexene acts as a cosolvent. The antisolvent effect of ethylene on the sorption of 1-hexene was found by Nath et al.,[24] with large error bounds on the results, but was clearly demonstrated with a more efficient molecular simulation technique by Banaszak et al.[16]

In this study, we measure the sorption isotherms of ethylene and 1-hexene and their mixture in three poly(ethylene-*co*-1-hexene) samples by a gravimetric method and supplement these measurements with the optical observation of swelling of polymer particles. The measurements were conducted in the region of typical reactor temperatures 70 and 90°C and above the melting temperatures of samples at 150°C. PC-SAFT predictions are compared with our sorption and swelling experimental data but the ability of PC-SAFT[29] is not newly developed in this study.

EXPERIMENTAL

LLDPE sample preparation

Polymerizations were conducted in a 1 L-stainless steel continuous gas-phase stirred bed reactor from Parr Instruments (Moline, IL) over a titanium-based Ziegler–Natta type catalyst. The entire reactor system is shown in Figure 1. Further details on the reactor system can be found in Han-Adebekun et al.[32] and Debling et al.[33] In all experiments, the total pressure was held constant at 120 psi (8.27 bar), and the reactor temperature was controlled at 70°C throughout the polymerization.

In addition to homopolymer, ethylene was also copolymerized at 2.00 and 3.25 mol % 1-hexene in the gas phase, which translated to 3.88 and 4.75 mol % 1-hexene in the polymer. For copolymerizations, the gas-phase composition was determined by FTIR (Galaxy 3000, Mattson IR). The comonomer injection rate was manipulated to control the gas comonomer composition at the desired level. After about 100–120 min, the polymerizations were stopped, and the polymer product was isolated for differential scanning calorimetry (DSC) analysis.

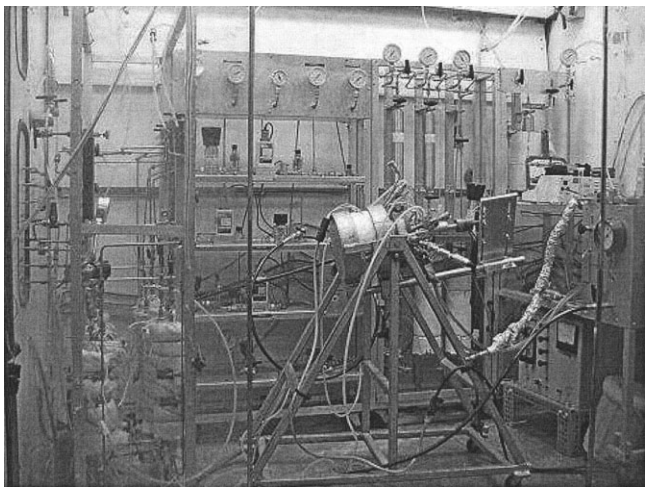

Figure 1 Gas-phase continuous stirred bed reactor system.

TABLE II
Characterization of Poly(ethylene-*co*-1-hexene) Samples

Sample	1-hexene in PE (mol %)	T_{melt} (°C)	Heat of fusion (J/g)	Crystallinity (wt %)
PE000	0.0	142.9	202.3	69.7–72.3
PE388	3.88	139.3	180.0	62.0–64.3
PE475	4.75	138.2	171.2	59.0–61.2

Crystallinity data is based on a value for the heat of fusion of 100% crystalline PE as 280–290 J/g.

DSC analysis was done using a device from TA Instruments (DSC Q100, New Castle, DE). For each measurement, one heating cycle was performed from 40 to 200°C at a heating rate of 10°C/min. Since the sample will recrystallize differently upon cooling, no further analysis was performed on a sample after the initial heating cycle. Melting points were determined by the peak of the melting exotherm curve and the heat of fusion required to melt a sample was determined by the area under the exotherm curve relative to the baseline heat flow.

Reported heats of fusion for 100% crystalline polyethylene vary greatly in the literature. To estimate a heat of fusion for 100% crystalline polyethylene, we measured the heats of fusion for PE's with M_w of 35,000 g/mol (polydispersity of 4.55) and 125,000 g/mol (HDPE with no polydispersity information) from Aldrich Chemicals. The density of these PE samples are well characterized and a degree of crystallinity can be estimated based on the assumption that the density of purely amorphous PE is 0.855 g/cm^3 and the density of purely crystalline PE is 1.00 g/cm^3 at 25°C.[34] The heat of fusion for 100% crystalline polyethylene for each PE sample is estimated by the measured heat of fusion divided by the calculated fraction of crystallinity determined by density data (i.e., the fraction of crystallinity is equal to the heat of fusion divided by the heat of fusion of 100% crystalline PE). Using this method, a range for the heat of fusion for 100% crystalline PE was determined to be 280–290 J/g. Table II summarizes the characteristics of the PE samples. The amount of 1-hexene incorporated into PE, the melting temperature, heat of fusion, and resulting crystallinity are indicated for the various PE samples. The results are based on the average of four DSC experiments for each PE type.

Gravimetric measurement of sorption isotherms

Sorption measurements were performed by gravimetric method using the pressure vessel attached to the magnetic suspension balance from Rubotherm GmbH (Bochum, Germany). The obtained gravimetric data were then corrected for buoyancy and for the effect of swelling of polymer samples. The apparatus used for gravimetic measurements is shown schematically in Figure 2 and consists of following principal parts: (i) pressure vessel of internal volume ~110 mL, equipped with the inlet and outlet fittings, temperature and pressure probes, (ii) on-line gas composition measurement and control system utilizing the mass spectrometer, (iii) magnetic suspension balance used for the measurement of dynamic changes of sample weight (with 0.01 mg resolution and 0.02 mg precision) at elevated temperatures (up to 150°C) and pressures (up to 50 bar), (iv) purification system for monomers and other gases, (v) temperature, pressure and mass flow control and measurement system, (vi) simple system for preparation of ethylene saturated by 1-hexene vapors in thermostated bubbled column, and (vii) industrial computer used for overall control and recording of measured data utilizing the LabView software from National Instruments (Austin, TX).

Experimental procedure of sorption measurements

Approximately 1 g of polymer particles was inserted into the weighing basket. The pressure vessel was hermetically closed, checked to be leak-proof, evacuated, and charged by the pure nitrogen at the temperature of sorption measurement. The sequence of measurements of the sample weight in the pure nitrogen at pressures 30, 25, 15, 5, and 0 bar was performed, to estimate the volume of the measured sample required for the buoyancy correction of the sample mass, cf. below. The weight of the sample as well as the temperature and pressure in the vessel were recorded at 10 s intervals during all measurements.

The pressure vessel was then evacuated and the ethylene was admitted into the vessel. The sequence of measurements in the pure ethylene at pressures 30, 25, 20, 15, 10, 5, and 0 bar was done to obtain sorption

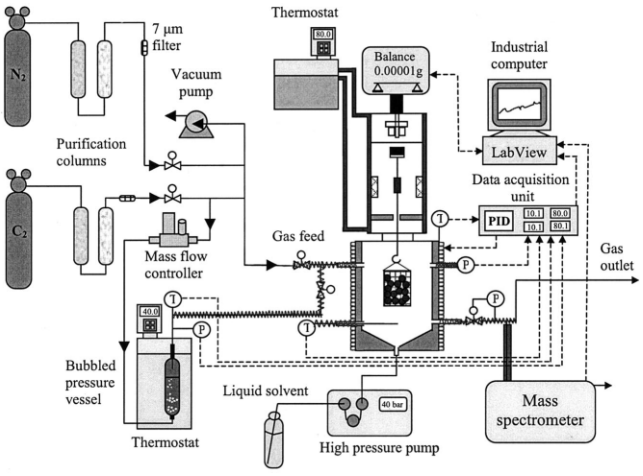

Figure 2 Scheme of the experimental equipment used for gravimetric sorption measurements of gases in polymers.

isotherm. When the thermodynamic equilibrium at the desired temperature and pressure has been established, the system has been retained at the equilibrium for at least 30 min.

The same procedure as for ethylene was then followed in 1-hexene sorption measurements, but the maximum pressure of 1-hexene was maintained below its vapor pressure. 1-hexene was fed into the pressure vessel as a liquid by means of a high-pressure pump, and it evaporated immediately after the injection into the thermostated pressure vessel.

The mixture of ethylene and 1-hexene was flowing continuously with flow rate 20 mL/min through the pressure vessel containing the weighed sample during cosorption measurements. The gas mixture of ethylene and 1-hexene was prepared in the column filled with liquid 1-hexene and bubbled by a continuous flow of ethylene. This bubbled column was thermostated and the control of its temperature and pressure allowed us to prepare gas mixture of the desired composition (i.e., 4.3 mol % of 1-hexene and 95.7 mol % of ethylene). The pressure in the bubbled column was the same as the pressure in the measuring sorption cell (i.e., 5, 10, 15, 20, or 25 bar). The temperature set point of the bubbled column was manipulated according to the gas composition analysis performed by the mass spectrometer.

Measurement of swelling of polymer samples

Volume changes of polymer samples caused by the sorption of penetrants are sometimes not mentioned in processing of gravimetric and permeation sorption measurements.[10] If the swelling is not neglected, then it is either predicted from equations of state[9,11] or it is measured by cathetometer as the dilatation of polymer films.[8,35] We employ the microscopy observation of changes of projected area of polymer particles caused by the sorption of penetrants.

The experimental equipment is shown in Figure 3 and is based on the visual observation of a polymer particle by microscope with attached digital camera. The central part of the apparatus is the small observation cell equipped with two glass windows with the diameter ~3 cm. The glass windows are kept in the distance 4 mm by a distance ring. The construction of the observation cell allows to conduct measurements both at high pressure (up to 30 bar) and vacuum conditions and is designed as self-sealing, i.e., high pressure makes the observation chamber hermetic due to pressing the glass windows against the O-rings placed in the metal part of the pressure cell. The observation cell of internal volume ~4 cm^3 is thermostated and is equipped with the inlet and outlet fittings, temperature and pressure probes. The particles are placed into the observation chamber between two glass windows and they are illuminated by a light source either from the top or from the bottom.

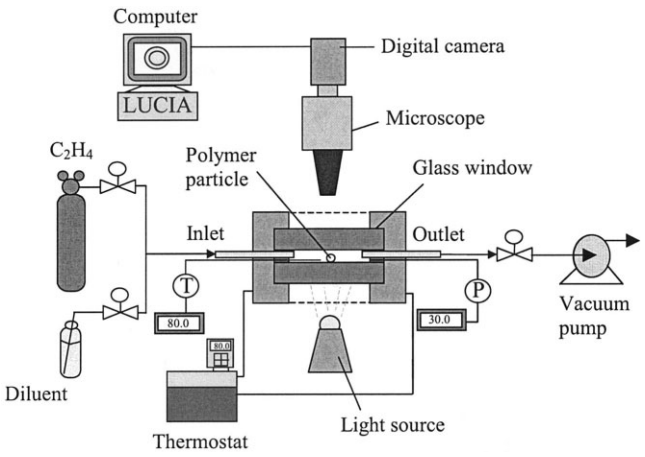

Figure 3 Scheme of the experimental equipment for the microscopic observation of the swelling of polymer particle.

The analysis of recorded images of the particle is carried out by the digital image-processing software LUCIA from Laboratory Imaging (Prague, Czech Republic). Changes in the area of particle image correspond to the particle dilatation (for sorption) or to the contraction (for desorption measurements). Experimental measurement of the polymer swelling can be employed to: (i) correct the gravimetric sorption measurement to the buoyancy force, (ii) estimate the density of system polymer-sorbed species, and (iii) study the dynamics of the sorption/desorption of the low-molecular weight components.

Experimental procedure of swelling measurements

Polymer particles are placed on the bottom glass in the observation cell, the cell is hermetically closed, and the particle having the sharpest contours is then selected for measurements. The cylindrical shield is installed around the observation cell and microscope to prevent the effects of ambient light sources on the quality of the image. The automatic capturing of the sequence of images at specified time intervals is set up in the LUCIA software. In the beginning of the experiment, several images are taken at vacuum conditions, and then ethylene or 1-hexene is admitted to the observation cell and the desired pressure is set. The sequence of swelling measurements at several pressures in the range 0–30 bar for ethylene and zero to vapor pressure for 1-hexene was performed. The processing of the recorded sequence of images allows checking the reaching of the swelling equilibrium. The setting of the microscope and the digital camera, i.e., focus and zoom, and the intensity of the light source were kept constant during the experiment.

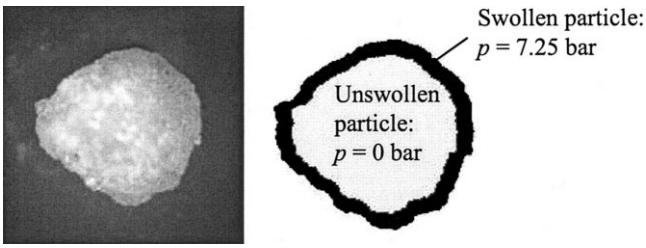

Figure 4 Original image of the LLDPE particle and the comparison of binarized images (overlaid) at the beginning (p = 0 bar) and at the end (p = 7.25 bar of 1-hexene) of the experiment at temperature 150°C.

The image processing consists of the binarization of the original image and characterization of the size of the particle by the equivalent diameter of the circle having the same area as the processed particle of irregular shape, cf. Figure 4. This sequence of processing with unchanged parameters was automatically repeated for the recorded sequence of images. The result of this processing is the evolution of the equivalent diameter of polymer particle during swelling/deswelling measurements. The relative change of the particle equivalent volume can be easily calculated from the third power of the change of the particle equivalent diameter.

Processing of Gravimetric Sorption Data

The measured weight of the polymer sample has to be corrected for the buoyancy and the effect of polymer swelling. The weighed object hooked up in the balance consists of: (i) approximately 1 g of the polymer, (ii) weighing basket, (iii) weighing hook, and (iv) some ballast weight. The balance reading provides the apparent measured weight $m_{\text{meas}}(p, T)$ at pressure p and temperature T, which has to be corrected for buoyancy of the measured object to obtain the true weight $m(p, T)$,

$$m = m_{\text{meas}} + \rho_{\text{gas}}(p,T)V(p,T) \tag{4}$$

where ρ_{gas} is the density of the gas phase calculated by the Lee-Kesler EOS,[36] and V is the volume of the measured object (comprising the volume of polymer and metal parts). The course of a typical equilibrium sorption measurement is displayed in Figure 5. The sorbed amounts displayed in this figure are already corrected for buoyancy force and scaled to the unit mass of amorphous fraction of polymer sample.

The volume V required in eq. (4) was determined by gravimetric measurements of the weighed object in nitrogen at constant temperature (e.g., at 90°C) at several pressures and at vacuum. The sorption of nitrogen in a polymer sample cannot be neglected; hence, a sorption isotherm of nitrogen in polyethylene reported by Maloney and Prausnitz[6] was employed.

$$\ln H_{N_2} = 7.49 + \frac{666}{T} \tag{5}$$

where H_{N_2} is the Henry's constant (in atm) and T is temperature (in K). The weight fraction of nitrogen in amorphous polyethylene w_{N_2} is determined as

$$w_{N_2} = p_{N_2}/H_{N_2} \tag{6}$$

where P_{N_2} is the pressure of nitrogen in atm. The difference of the weight of measured object at vacuum conditions and at elevated pressures in nitrogen is

$$m_{\text{meas}}(0\ \text{bar},T) - m_{\text{meas}}(P_{N_2},T) = \rho_{\text{gas}}(P_{N_2},T)V - w_{N_2}(P_{N_2},T)m_{\text{amPol}} \tag{7}$$

where m_{meas} is the balance reading at specified conditions and $m_{\text{am.Pol.}}$ is the weight of amorphous fraction of the polymer sample calculated at 70 and 90°C as

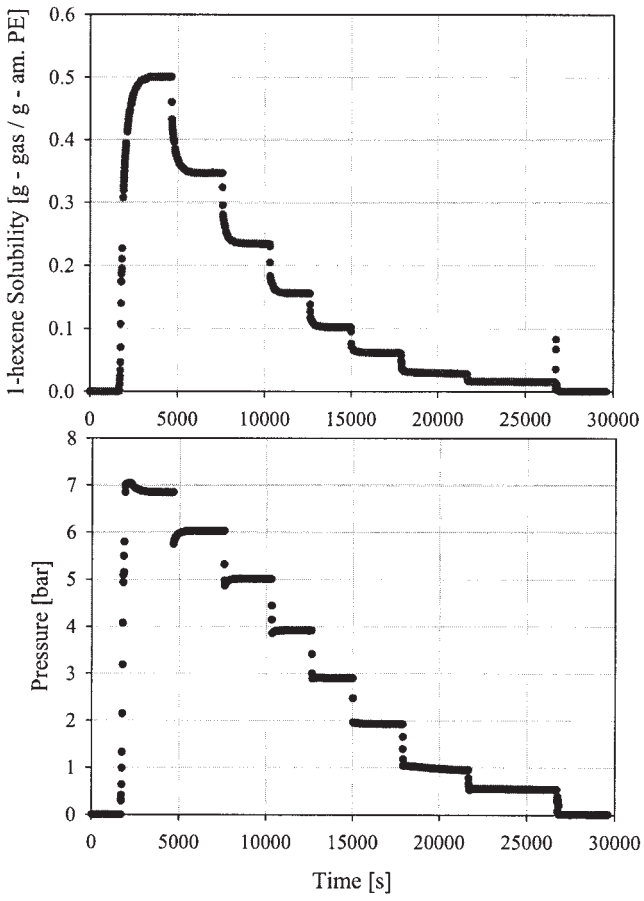

Figure 5 The course of a typical sorption measurement—the dynamics of sorption/desorption of 1-hexene in sample PE000 at 150°C.

$$m_{\text{amPol}} = w_{\text{amPol}} m_{Pol} \tag{8}$$

where $m_{\text{Pol.}}$ is the weight of polymer sample, and the weight fraction of amorphous phase $w_{\text{am.Pol.}}$ is determined from the crystallinity χ_{cr} (i.e., the mass fraction of crystalline phase) of the polymer sample.

$$w_{\text{amPol}} = (1 - \chi_{\text{cr}}) \tag{9}$$

At 150°C, that is, above the melting point of polyethylene, the weight of amorphous fraction of polymer $m_{\text{am.Pol.}}$ is equal to the weight of polymer sample m_{Pol}. We search for the best volume V to fit set of eq. (7) for $P_{N_2} = 5$, 15, 25 and 30 bar, respectively. The volumes V at temperatures 70, 90, and 150°C are different because of changes in polymer density.

When the nitrogen solubility in polyethylene described by eqs. (5) and (6) is neglected the estimated volume V of measured object is smaller than it actually is. The discrepancy caused by neglecting the nitrogen solubility in polyethylene is up to 20% in the case of ethylene solubility and <1% in the case of 1-hexene solubility.

The results of gravimetric sorption measurements have to be corrected not only for the buoyancy of the measured sample, but also for the buoyancy of the swollen volume of the measured polymer. Thus, eq. (4) can be rewritten in an alternative form

$$m = m_{\text{meas}} + \rho_{gas}(p,T)(V(0,T) + \Delta V_{\text{swell}}) \tag{10}$$

where

$$\Delta V_{\text{swell}} = V(p,T) - V(0,T) = V_{\text{am}}(p,T) - V_{\text{am}}(0,T) \tag{11}$$

where the swelling ΔV_{swell} is caused by the sorption of penetrant species into the amorphous fraction of polymer sample.

The sorption data of all samples were corrected for the buoyancy of the swollen volume using the results of swelling measurements made with corresponding samples. The swelling data of samples PE000, PE388, and PE475 varied only slightly and, therefore, we report only swelling data for the sample PE388 in Figure 6. Because of the uncertainty of the measured swelling and implied uncertainty in the correction for the buoyancy due to the swollen volume, the error of evaluated solubilities is 1% for ethylene and 0.2% for 1-hexene (the percentage is related to the penetrant solubility in the polymer).

PC-SAFT predictions for polymer swelling

In this study, the swelling was determined either from direct microscopy observations or was estimated from the PC-SAFT EOS.[29–31] All our calculations with PC-SAFT EOS were conducted with parameters determined by Banaszak et al.[16] for linear polyethylene by fitting the results of molecular simulations. Banaszak et al.[16] also found that the homopolymer PC-SAFT EOS is equally predictive for LLDPEs with up to 5 mol % 1-hexene content as a comonomer. Generally one of the goals of this study is to compare PC-SAFT predictions with our experimental findings, but the ability of PC-SAFT[29] is not newly developed. The effect of crystallites is incorporated into PC-SAFT in our earlier publication by Banaszak et al.[16]

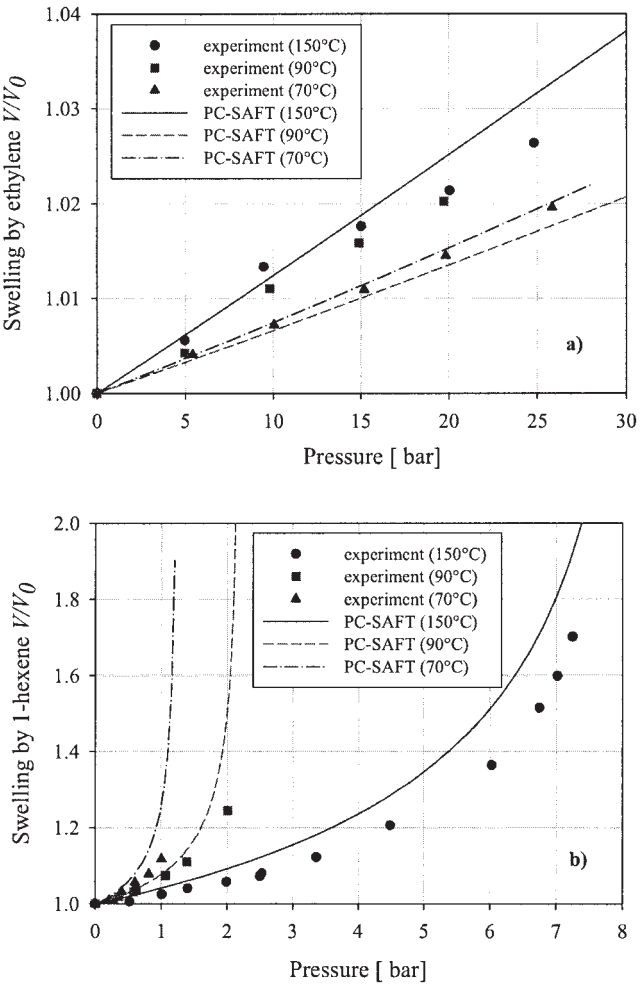

Figure 6 Swelling of the LLDPE particle (sample PE388) by: (a) ethylene and (b) 1-hexene at 70, 90, and 150°C. V/V_0 is the ratio of volumes of the swollen and unswollen polymer particle. The points are experimental results of swelling and the curves are the PC-SAFT predictions.

To estimate the swelling of amorphous polymer from the PC-SAFT EOS, the equilibrium composition of the amorphous polymer has to be calculated first. The volume of amorphous polymer at vacuum conditions $V_{\text{am}}(0,T)$ is calculated as

$$V_{\text{am}}(0,T) = \frac{m_{\text{amPol}}}{\rho_{\text{am}}(0,T)} \tag{12}$$

TABLE III
Pure Component PC-SAFT Parameters

Component	m	σ (Å)	ε/k (K)
Ethylene	1.5930	3.4450	176.47
1-hexene	2.9853	3.7753	236.81
PE	2633.8	3.9876	246.00

where the density of amorphous polymer $\rho_{am}(0, T)$ is calculated from the PC-SAFT EOS. The volume $V_{am}(p,T)$ is calculated as

$$V_{am}(p,T) = \frac{m_{amPol}\left(1 + \sum_i W_i\right)}{\rho_{am}(p,T,W_i)} \quad (13)$$

where $\rho_{am}(p,T,W_t)$ is the density of amorphous polymer phase in equilibrium with gas at pressure p and composition W_i, where W_i is the relative weight fraction of the i-th penetrant in the amorphous polymer. Both $\rho_{am}(p,T,W_i)$ and W_i were estimated from PC-SAFT.

The pure component PC-SAFT parameters are: (i) segment diameter σ, (ii) the number of segments per molecule m, and (iii) the segment energy ε/k. These parameters were taken from Banaszak et al.[16] and are summarized in Table III. The parameter $m = 2633.8$ for polyethylene corresponds to the selected average molecular weight M_w = 100,000 g/mol because beyond this molecular weight no significant changes in density and gas sorption predictions are observed.

The binary interaction parameters k_{ij} were estimated by fitting the PC-SAFT to binary equilibrium data ethylene/polyethylene and 1-hexene/polyethylene at 150°C and they are reported in Table IV. Parameters k_{ij} are assumed to be temperature-independent in this work and were used for predictions of sorption data at temperatures 70, 90, and 150°C. The same binary interaction parameters k_{ij} were also used in the case of ternary system ethylene/1-hexene/polyethylene, and the remaining k_{ij} parameter for ethylene/1-hexene was set to zero.

Although the swelling of polyethylene samples in 1-hexene is more extensive than that in ethylene, the correction of gravimetric ethylene sorption data for buoyancy of the swollen volume given by eq. (10) is more important than in the case of 1-hexene. The relative correction of gravimetric sorption data to swelling is up to 20% in the case of ethylene sorption and up to 3% in the case of 1-hexene sorption over the measured pressure and temperature ranges.

RESULTS AND DISCUSSION

Swelling of LLDPE sample

Swelling measurements of sample PE388 in ethylene and 1-hexene conducted at 70, 90, and 150°C are summarized in Figure 6 and compared with predictions of the PC-SAFT EOS. The quantity V/V_0 is the ratio of volumes of swollen and unswollen semicrystalline polymer particle. The swelling by ethylene at 150°C is larger than swelling at 70 or 90°C because the entire polymer sample is amorphous at conditions above its melting point. The swelling measurements were conducted with one porous polyolefin particle, and we verified that the presence of pores has no significant effect on the reported results of swelling measurements.

The results presented in Figure 6 show that the swelling estimated using PC-SAFT EOS is generally higher than our experimental results for both ethylene and 1-hexene. Only in the case of ethylene sorption at 90°C is the swelling estimated using the PC-SAFT, lower than that measured experimentally. Our measured swelling data are in a good agreement with results of dilatation measurements reported by Moore and Wanke.[8] The significant swelling estimated by the PC-SAFT, especially in the case of 1-hexene sorption at temperatures below 100°C, was compared by Banaszak et al.[16] to the estimate obtained by molecular simulations.

The experimentally measured swelling data were used for corrections of gravimetric solubility data for the buoyancy of the swollen volume, cf. eq. (10). The swelling measurements were not done for ethylene/1-hexene mixture, because our swelling apparatus is not equipped with a reliable control of the gas-phase composition. The selective condensation of 1-hexene at cold spots of the observation cell can happen. Therefore, the volume ΔV_{swell} required to correct the gravimetric cosorption measurements was estimated as the sum of swellings of pure ethylene and 1-hexene corresponding to their partial pressures.

Sorption of pure ethylene and 1-hexene in LLDPE

Sorption isotherms for pure ethylene and 1-hexene in the sample PE388 measured at 70, 90, and 150°C are reported in Figure 7. Each experimental point in this Figure was calculated from the average value of ~200 balance readings recorded over the period of ~40 min of measurements at equilibrium conditions. The amount of sorbed ethylene in LLDPE sample PE388 is directly proportional to ethylene pressure p_{Eth} in the considered range of pressures. Hence, the solubility of

TABLE IV
Binary Interaction Parameters k_{ij} Used in the PC-SAFT Modeling

k_{ij}	1-hexene	PE
Ethylene	0.00	0.03
1-hexene		0.00

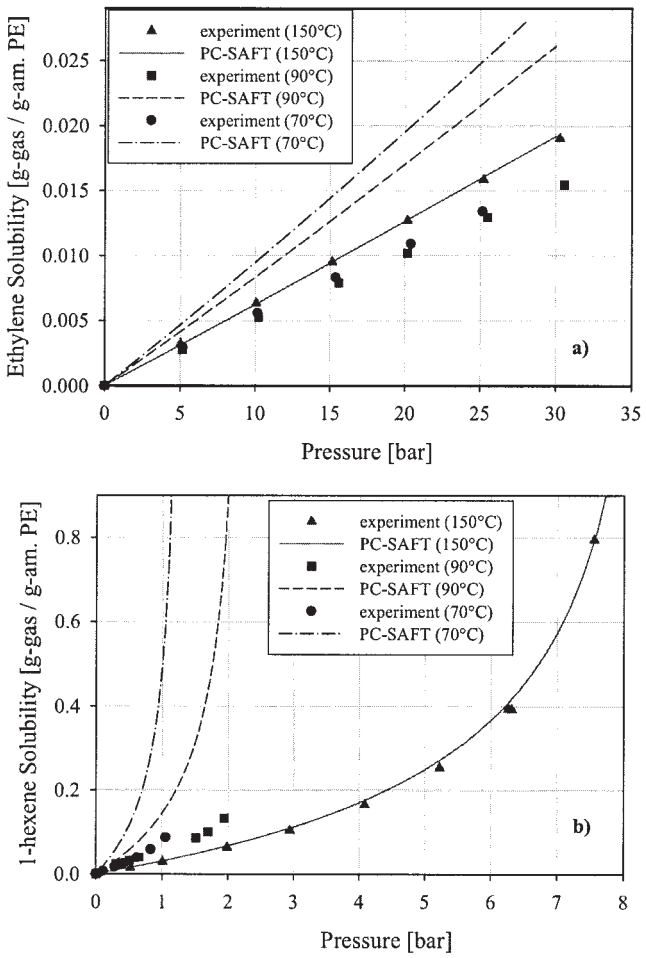

Figure 7 Gas solubilities in LLDPE (Sample PE388): (a) sorption of ethylene, (b) sorption of 1-hexene at 70, 90, and 150°C. The points are sorption measurements and the curves are PC-SAFT predictions.

ethylene in polymer sample can be described by Henry's law

$$S_{\mathrm{Eth}} = H_{\mathrm{Eth}}(T)p_{\mathrm{Eth}} \tag{14}$$

where $H_{\mathrm{Eth}}(T)$ is temperature-dependent Henry's law constant obtained from the slope of corresponding sorption isotherm and S_{Eth} is the solubility (in $g_{\mathrm{Eth}}/g_{\mathrm{am.\ Pol.}}$) of ethylene in the amorphous phase of poly(ethylene-*co*-1-hexene) sample.

Sorption isotherms of 1-hexene are nonlinear and their slopes gradually increase at elevated pressures at all considered temperatures, cf. Figure 7(b). The solubility of 1-hexene in polymer is at least about an order of magnitude larger than the solubility of ethylene at the same temperature and pressure.

The PC-SAFT EOS was used to predict the sorption equilibrium of pure ethylene and 1-hexene in polyethylene. The binary interaction parameter k_{ij} for each pair of components was determined by fitting the PC-SAFT prediction to sorption isotherms at 150°C in purely amorphous (melted) polymer, cf. Table IV. PC-SAFT EOS largely overpredicts the solubility of both ethylene and 1-hexene in considered LLDPE sample at 70 and 90°C. This discrepancy of predicted and measured solubilities is caused by elastic constraints

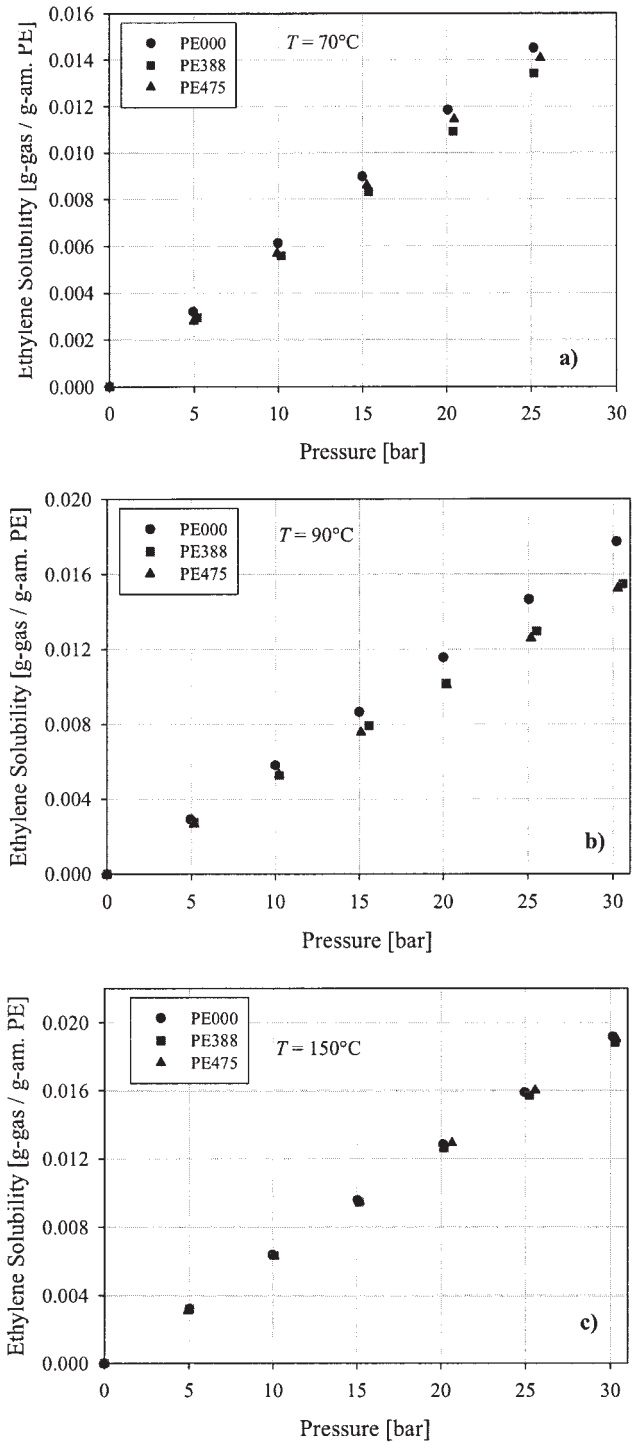

Figure 8 Ethylene solubility in poly(ethylene-*co*-1-hexene) samples PE000, PE388, PE475 at: (a) 70°C, (b) 90°C, and (c) 150°C.

within the amorphous polymer phase of semicrystalline polymer that inhibit the sorption in the amorphous phase, cf. detailed description of this effect by Banaszak et al.[16]

Figures 8 and 9 summarize the measured solubilities of pure ethylene and 1-hexene in the three investigated LLDPE samples at temperatures 70, 90, and 150°C, listed in Table II. No significant effect of short chain branching, i.e., of content of 1-hexene comonomer in the polymer, is observed in experimental results. This observation is in a good agreement with results of molecular simulations of Banaszak et al.[16] who simulated the sorption of ethylene and 1-hexene in the same samples of poly(ethylene-*co*-1-hexene).

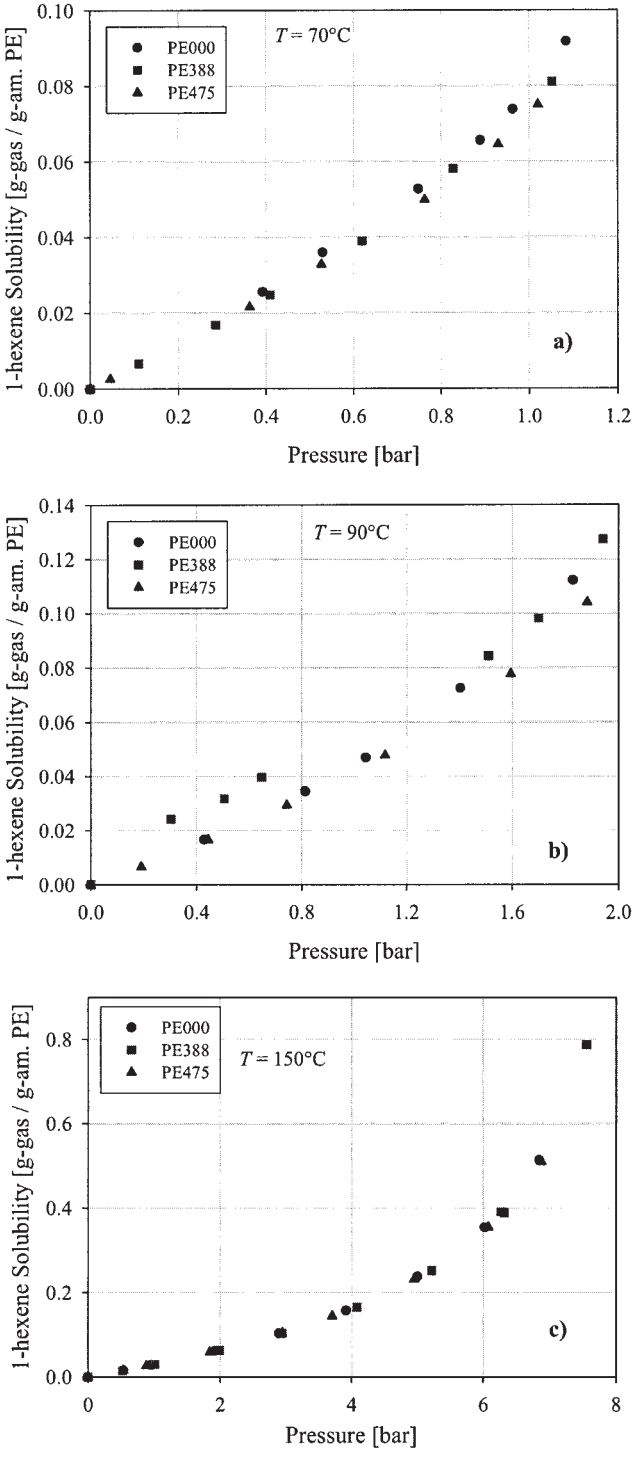

Figure 9 1-hexene solubility in poly(ethylene-*co*-1-hexene) samples PE000, PE388, PE475 at: (a) 70°C, (b) 90°C, and (c) 150°C.

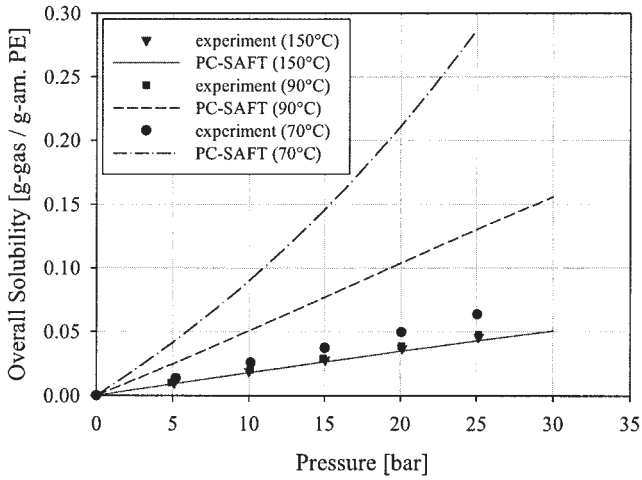

Figure 10 Overall solubility of ethylene/1-hexene gas mixture in LLDPE (Sample PE388) at 70, 90, and 150°C. The points are experimental results and the curves are the PC-SAFT predictions. The gas phase composition is 95.7 mol % ethylene/4.3 mol % 1-hexene for all measurements.

Cosorption of 1-hexene and ethylene in LLDPE

Cosorption isotherms of ethylene/1-hexene mixture in LLDPE samples were measured at the same temperatures 70, 90, and 150°C as pure components. The composition of the gas mixture was the same (4.3 mol % of 1-hexene and 95.7 mol % of ethylene) in all cosorption measurements and was analyzed by an online connected mass spectrometer.

Cosorption isotherms of ethylene/1-hexene gas mixture in PE388 sample are presented in Figure 10 together with predictions of PC-SAFT EOS. The binary interaction parameters k_{ij} fitted previously to measured sorption isotherms of ethylene/LLDPE and 1-hexene/LLDPE at 150°C were employed also in calculations of the mixture ethylene/1-hexene/LLDPE. PC-SAFT fits the experimental data well above the melting point with very little adjusting of the only binary parameter k_{ij} for ethylene/polyethylene mixture. The solubility of ethylene/1-hexene mixture in LLDPE at temperatures 70 and 90°C predicted by PC-SAFT EOS is significantly larger than experimental data.

Figure 11 compares the overall solubility of ethylene/1-hexene mixture with a simple summation of

solubilities of pure components at their partial pressures and demonstrates the so-called antisolvent effect observed at temperatures below the melting point of polymer. The sum of solubilities of pure components S_{mix} is represented by the full line in Figure 11 and is calculated as

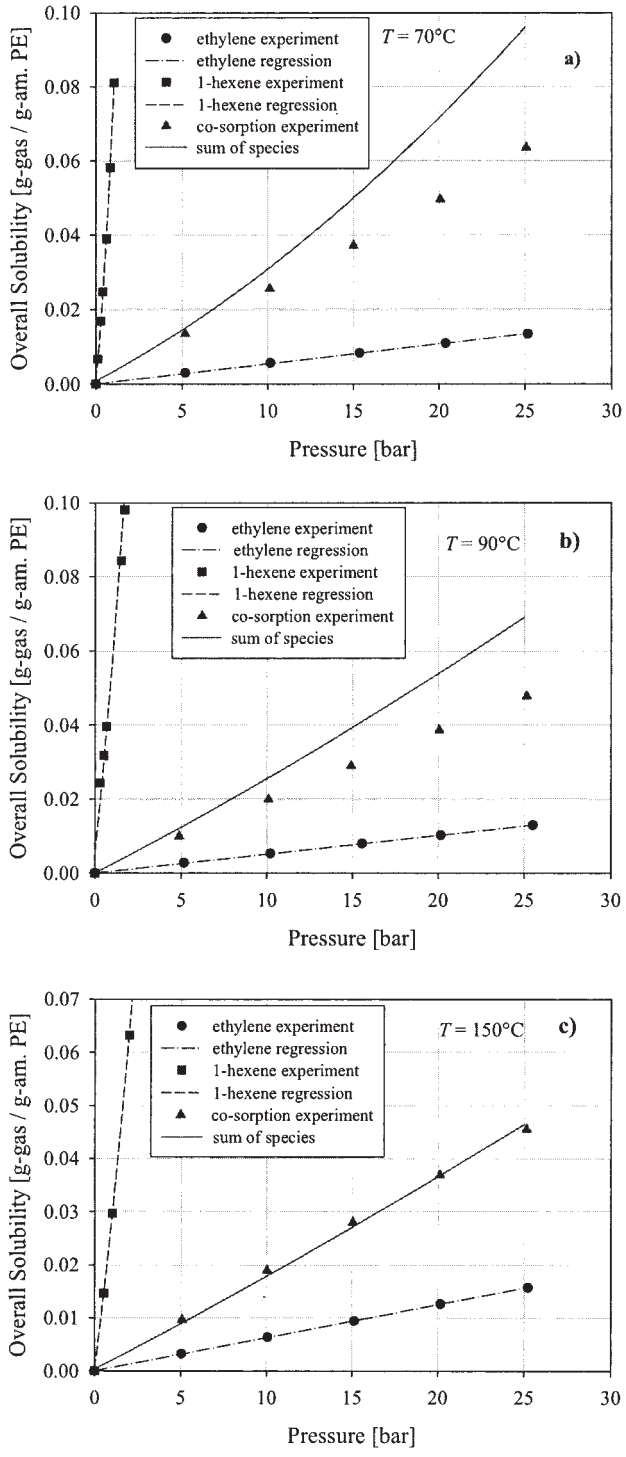

Figure 11 Cosorption effect of the ethylene/1-hexene mixture in LLDPE (Sample PE388) at temperatures: (a) 70°C, (b) 90°C and (c) 150°C. The gas phase composition is 95.7 mol % ethylene/4.3 mol % 1-hexene for all conditions.

TABLE V
PC-SAFT Prediction of the Antisolvent Effect of Ethylene and the Cosolvent Effect of 1-hexene for Sorption in the Sample PE388 at 90°C

Component	Pure component sorption S_i (g-gas/g-am.pol.)	Cosorption S_i (g-gas/g-am.pol.)
Ethylene		
P_{Eth} = 23.25 bar	0.0199	0.0277
1-hexene		
P_{Hex} = 1.075 bar	0.1633	0.1013

$$S_{mix} = H_{Eth}(T) \cdot p_{Eth} + (a(T) \cdot p_{Hex} + b(T) \cdot p_{Hex}^2) \quad (15)$$

where H_{Eth} is the Henry's law constant for ethylene, $a(T)$ and $b(T)$ are parameters of the nonlinear sorption isotherm of 1-hexene and p_{Eth} and p_{Hex} are the partial pressures of ethylene and 1-hexene, respectively. It is observed that the measured cosolubility of the gas mixture is smaller than that predicted from independent sorption measurements of pure components S_{mix}. PC-SAFT predictions show that the ethylene solubility is enhanced by the addition of 1-hexene to the gas phase, so that 1-hexene acts as a cosolvent agent. This cosolvent effect was also confirmed by the molecular simulations of Banaszak et al.[16] On the contrary, the addition of ethylene to the gas phase lowers the 1-hexene solubility in LLDPE, and ethylene, thus, acts as an antisolvent agent. The PC-SAFT predictions for solubility of pure ethylene and pure 1-hexene as well as the solubility of these components in the mixture at the same partial pressure and temperature are summarized in Table V. The decrease of 1-hexene solubility is larger than the increase of ethylene solubility and, therefore, the overall solubility of the gas mixture is lower than the calculated solubility S_{mix} corresponding to the sum of pure component solubilities. The difference between the measured solubility of ethylene/1-hexene mixture in LLDPE and the calculated solubility S_{mix} is large especially at lower temperatures and it disappears at 150°C.

Experimentally measured solubility data of ethylene/1-hexene mixture in all three LLDPE samples are summarized in Figure 12. The solubility of gas mixture in the homopolymer sample PE000 is slightly larger than that in PE388 and PE475 samples at 70 and 90°C, cf. Figure 12(a,b).

CONCLUSIONS

Equilibrium sorption isotherms of ethylene, 1-hexene, and ethylene/1-hexene mixture in three samples of poly(ethylene-*co*-1-hexene) with different content of 1-hexene were determined gravimetrically both below (at 70 and 90°C) and above the melting point (at 150°C) of polymer. The volumetric swelling of inves-

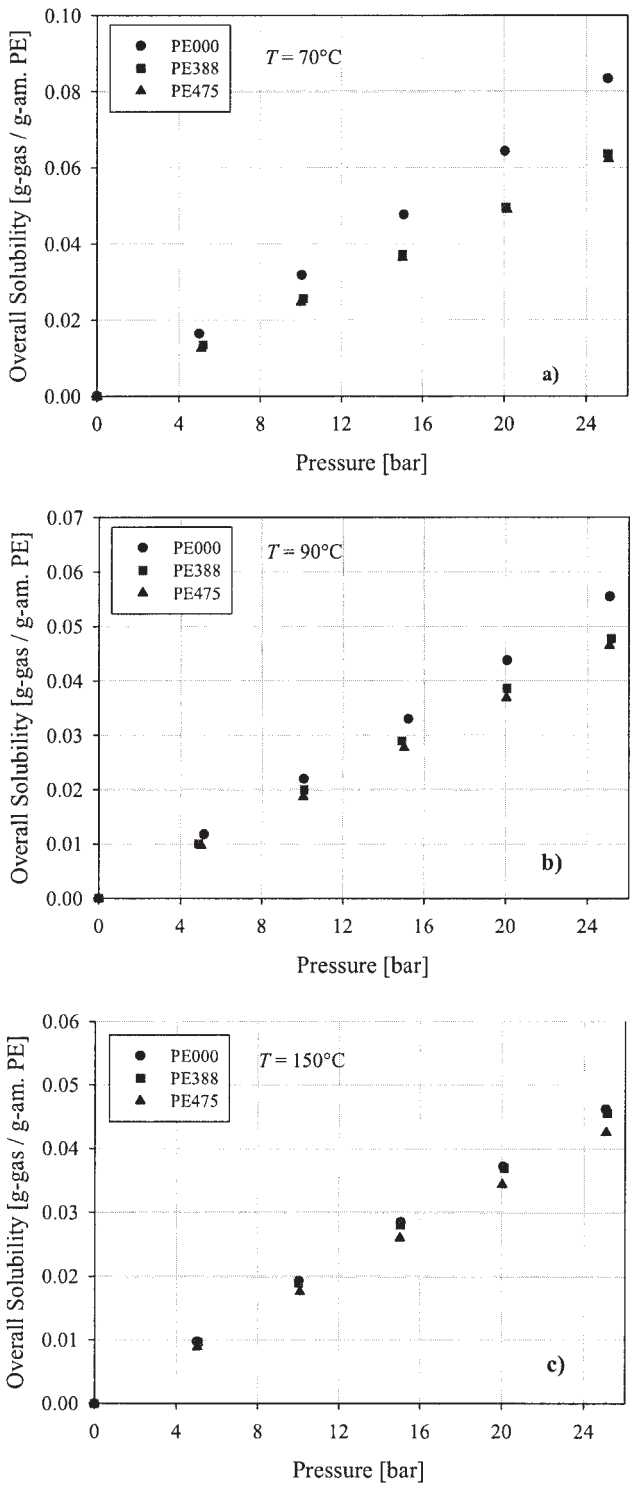

Figure 12 Overall solubility of ethylene/1-hexene mixture in poly(ethylene-*co*-1-hexene) samples PE000, PE388, PE475 at temperatures: (a) 70°C, (b) 90°C, and (c) 150°C. The gas-phase composition is 95.7 mol % ethylene/4.3 mol % 1-hexene for all conditions.

tigated samples caused by the sorption of penetrants was measured microscopically, and the obtained swelling data were employed in the correction of gravimetric data for the buoyancy of the swollen volume.

The obtained sorption isotherms show clearly the reduced solubility of penetrants in the amorphous phase of semicrystalline polymers at temperatures below their melting points when compared with theoretical predictions. Results of cosorption measurements of ethylene/1-hexene mixture indicate that the solubility of mixture is smaller than the sum of solubilities of individual components at their respective partial pressures. The simulations of cosorption by PC-SAFT EOS indicate that 1-hexene enhances the solubility of ethylene and, thus, acts as a cosolvent, but ethylene decreases the solubility of 1-hexene considerably and, thus, acts as an antisolvent agent. Short chain branching of investigated LLDPE samples (i.e., the content of 1-hexene monomeric units) has only small effect on the solubility of penetrants.

PC-SAFT EOS generally overpredicts the volumetric swelling of LLDPE samples caused by the sorption, especially in the case of 1-hexene. PC-SAFT also overpredicts the solubility of ethylene and 1-hexene in LLDPE samples below the melting point. Another limitation of PC-SAFT with semicrystalline polymers is the description of the density increase of amorphous phase (swelled by penetrants) due to the crystalline constraints. Banaszak et al.[16] improved the quality of PC-SAFT predictions by considering the fraction of elastically affected chains in the semicrystalline polymer.

NOMENCLATURE

Symbols
Abbreviations Description

$c_M^{\text{am.pol.}}$	Concentration of monomer in the amorphous polymer phase (mol m^{-3})
c_M^{bulk}	Bulk concentration of monomer (mol m^{-3})
E_a	Activation energy (J mol^{-1})
E'_a	Apparent activation energy (J mol^{-1})
H_{Eth}	Henry's constant of ethylene in amorphous polymer (g-gas/(g-am.PE. bar))
H_{N_2}	Henry's constant of nitrogen in amorphous polymer (atm)
k_{ij}	Binary interaction parameters
k_{p0}	Preexponential factor
k'_{p0}	Apparent preexponential factor
m	Weight of the measured object corrected for buoyancy and swelling (g)
m	The number of segments per molecule
m_{amPol}	Weight of amorphous fraction of the polymer sample (g)
m_{meas}	Weight of balance reading (g)
m_{Pol}	Weight of polymer sample (g)
M_w	Average molecular weight (kg mol^{-1})
p	Pressure in the sorption cell (bar)

p_i	Partial pressure of penetrant (bar)
R	Gas constant (8.314 J mol^{-1} K^{-1})
R_p	Chain propagation (mol m^{-3} s^{-1})
S_i	Solubility of penetrant in amorphous polymer phase ($g_{gas}/g_{am.PE}$)
T	Temperature (K)
T_{melt}	Melting temperature (°C)
V	Volume of the measured object (m^3)
V_{am}	Volume of amorphous polymer (cm^3)
w_{amPol}	Weight fraction of amorphous phase in semicrystalline polymer
w_i	Weight fraction of penetrant in amorphous polymer phase
W_i	Relative weight fraction of penetrant in the amorphous polymer
χ_{cr}	Crystallinity
ΔV_{swell}	Swelling (cm^3)
ε/k	The segment energy (K)
ρ_{am}	The density of amorphous polymer (g cm^{-3})
ρ_{gas}	Density of the gas phase (g cm^{-3})
σ	Segment diameter (Å)

References

1. Ivanchev, S. S.; Kryzhanovskii, A. V.; Gapon, I. I.; Ponomareva, Ye. L. Polymer Science USSR 1990, 32, 64.
2. Karol, F. J; Kao, S.-C.; Cann, K. J. J Polym Sci Part A: Polym Chem 1993, 31, 2541.
3. Hutchinson, R. A.; Chen, C. M.; Ray, W. H. J Appl Polym Sci 1992, 44, 1387.
4. Michaels, A. S.; Bixler, H. J. J Polym Sci 1961a, 50, 393.
5. Michaels, A. S.; Bixler, H. J. J Polym Sci 1961b, 50, 413.
6. Maloney, D. P.; Prausnitz, J M. AIChE J 1976, 22, 74.
7. Kamiya, Y.; Hirose, T.; Mizoguchi, K.; Naito, Y. J Polym Sci Part B: Polym Phys 1986, 24, 1525.
8. Moore, S. J.; Wanke, S. E. Chem Eng Sci 2001, 56, 4121.
9. Sato, Y.; Fujiwara, K.; Takikawa, T.; Takishima, S.; Masuoka, H. Fluid Phase Equilibria 1999, 162, 261.
10. Yoon, J.-S.; Yoo, H.-S.; Kang, K.-S. Eur Polym J 1996, 32, 1333.
11. Sato, Y.; Tsuboi, A.; Sorakubo, A.; Takishima, S.; Masuoka, H.; Ishikawa, T. Fluid Phase Equilibria 2000, 170, 49.
12. Hutchinson, R. A.; Ray, W. H. J Appl Polym Sci 1990, 41, 51.
13. Michaels, A. S.; Hausslein, R. W. J Polym Sci Part C 1965, 61, 61.
14. Doong, S.; J; Ho, W. S. W. Ind Eng Chem Res 1991, 30, 1351.
15. Kiparissides, C.; Dimos, V.; Boultouka, T.; Anastasiadis, A.; Chasiotis, A. J Appl Polym Sci 2003, 87, 953.
16. Banaszak, B. J.; Lo, D.; Widya, T.; Ray, W. H.; de Pablo, J. J.; Novak, A.; Kosek J. Macromolecules 2004, 37, 9139.
17. Yoon, J.-S.; Chung, C.-Y.; Lee, I.-H. Eur Polym J 1994, 30, 1209.
18. Robeson, L. M.; Smith, T. G. J Appl Polym Sci 1968, 12 2083.
19. Li, N. N.; Long, R. B. AIChE J 1969, 15, 73.
20. Dörr, H.; Kinzl, M.; Luft, G. Fluid Phase Equilibria 2001, 178, 191.
21. Kennis, H. A. J.; de Loos, Th. W.; de Swaan Arons, J. Chem Eng Sci 1990, 45, 1875.
22. Chan, A. K. C.; Radosz, M. Macromolecules 2000, 33, 6800.
23. Chen, X.; Yasuda, K.; Sato, Y.; Takishima, S.; Masuoka, H. Fluid Phase Equilibria 2004, 215, 105.
24. Nath, S. K.; Banaszak, B. J.; de Pablo, J. J. Macromolecules 2001, 34, 7841.
25. Chapmann, W. G.; Gubbins, K. E.; Jackson, G.; Radosz, M. Fluid Phase Equilibria 1989, 52, 31.
26. Chapmann, W. G.; Gubbins, K. E.; Jackson, G.; Radosz, M. Ind Eng Chem Res 1990, 29, 1709.
27. Huang, S. H.; Radosz, M. Ind Eng Chem Res 1990, 29, 2284.
28. Huang, S. H.; Radosz, M. Ind Eng Chem Res 1991, 30 1994.
29. Gross, J.; Sadowski, G. Ind Eng Chem Res 2001, 40, 1244.
30. Gross, J.; Sadowski, G. Ind Eng Chem Res 2002, 41, 1084.
31. Tumakaka, F.; Gross, J.; Sadowski, G. Fluid Phase Equilibria 2002, 194–197, 541.
32. Han-Adebekun G. C.; Debling, J. A.; Ray, W. H. J Appl Polym Sci 1997, 64, 373.
33. Debling, J. A.; Ray, W. H. Ph.D. Dissertation, University of Wisconsin-Madison, 1997.
34. Brandrup, J.; Immergut, E. H.; Grulke, E. A. Polymer Handbook, 4th ed.; Wiley: New York, 1999.
35. Sato, Y.; Yurugi, M.; Yamabiki, T.; Takishima, S.; Masuoka, H. J Appl Polym Sci 2001, 79, 1134.
36. Reid, R. C.; Prausnitz, J. M.; Poling, B. E. The Properties of Gases and Liquids, 4th ed., McGraw-Hill: New York, 1987.